# Electrooptic Studies on Polymer-Dispersed Liquid-Crystal Composite Films. III. Poly(methyl methacrylate-*co*-butyl acrylate)/E7 and Poly(methyl methacrylate-*co*-butyl acrylate)/E8 Composites

**A. K. Kalkar, V. V. Kunte, S. A. Bhamare**

*Department of Physics, Institute of Chemical Technology, University of Mumbai, Mumbai 400019, India*

Received 19 July 2006; accepted 1 February 2007
DOI 10.1002/app.27132
Published online 25 September 2007 in Wiley InterScience (www.interscience.wiley.com).

**ABSTRACT:** Composite films composed of poly(methyl methacrylate-*co*-butyl acrylate) (PMMABA) and nematic-type liquid crystals E7 and E8 (commercial products from E. Merck, Darmstadt, Germany) were prepared through solvent casting in chloroform. The morphology and electrooptic responses were studied. Scanning electron microscopy observations showed that the liquid-crystal phase (E7 or E8), as larger, elongated, interconnected cavities, was continuously embedded in a spongelike PMMABA matrix. At a specific level of the liquid-crystal (E7 or E8) loading (30/70 wt %), the effects of the voltage, temperature, and frequency of an applied alternating-current electric field on the transmittance of the composite films were measured with a He–Ne laser (wavelength = 632.8 nm). The results were interpreted in terms of the aggregation structure, interfacial interaction, and solubility of the liquid crystal in the matrix polymer. The results indicated that, under these experimental conditions, the output could be controlled to a desired level by the selection of suitable liquid crystals to prepare polymer-dispersed liquid-crystal, electrooptic, active composite films with a response time of the order of only milliseconds or less.  J Appl Polym Sci 107: 689–699, 2008

**Key words:** coatings; composites; crystal structures; electron microscopy; films

## INTRODUCTION

Polymer-dispersed liquid crystals (PDLCs) have attracted much attention recently as novel electronic materials for a wide variety of electrooptic applications ranging from switchable windows[1–4] to high-resolution active matrix projection displays,[5–9] projection light valves,[10–12] and switching gratings.[13,16]

This research is directed toward developing novel device concepts with advanced optical materials particularly related to optical information storage and switching. In this direction, stressed liquid-crystal (LC) films consisting of unidirectionally oriented domains of LC separated with polymer chains have been developed more recently.[17] These PDLC films eliminate light scattering, produce a large electrically controlled shift in the refractive index, and switch with submillisecond speed; major applications of these new electrooptic materials are in electrically controlled phase retardation devices, which include high-speed displays, beam-steering devices, and light modulators.[17–22] Similarly, West et al.[23] at Kent developed a new flexible, bistable, smectic A–LC/polymer, electrooptic composite material. This new material has high potential in large-area, high-resolution, and wide-angle display applications with sunlight readability.

In a PDLC film, an LC material is embedded in an isotropic polymer matrix in the form of droplets of micrometer to submicrometer size. Then, the film is electrically driven by being sandwiched between two conducting electrodes. However, each specific application has its own electrical constraints, such as the on driving voltage, power consumption, and frequency of operation. Nevertheless, these PDLC films still have the advantage that they draw very little current ($\mu A/cm^2$) and consume little electric power.[24] The operational principle of these PDLC films is based on electric-field-controlled light scattering from the optical microstructure heterogeneities and/or homogeneities produced because of LC droplets. The spatial distortion of LC nematic directors induced by the randomly oriented polymer network/polymer walls in composite PDLC films and mismatch of the refractive indices between the polymer and LC are the origins of the light scattering.[25–27] The distortion of nematic directors in LC droplets/channels and therefore the high scattering and

*Correspondence to:* A. K. Kalkar (kalkarak@udct.org).
Contract grant sponsor: University Grants Commission (New Delhi, India); contract grant number: F540/1/CAS/2000 (SAP-1)/28.3.00.

switching properties of PDLC films are strongly dependent on the aggregation structure of the composite films. The aggregation structure, in terms of the size of the LC droplets and channels, can be controlled on the basis of the solvent evaporation rate and the component ratio during the film preparation process.[28,29] In fact, through the control of these experimental conditions, a wide variety of morphologies can be generated, ranging from spherical droplets to continuous channels. Drzaic[30] investigated the effects of the domain size on the switching field and showed that this field is inversely proportional to the average domain size and the domain anisotropy. In addition to this, the electrooptic responses of LC molecules are strongly dependent on the anchoring conditions of the LC molecules on the surface of the polymer cavity surrounding a LC droplet.[25] However, considerable research is still needed to understand and optimize the properties of PDLC films.

In a continuation of our earlier work,[31,32] in this article we discuss the electrooptic light scattering properties of poly(methyl methacrylate-*co*-butyl acrylate) (PMMABA)/E7 and PMMABA/E8 PDLC films on the basis of the aggregation structure of the PMMABA/LC composite film and the effects of aggregation states of the composite films such as the size of LC domains and the compatibility between the matrix polymer (PMMABA) and LC (E7 or E8) on electrooptic properties such as the driving voltage and response speeds. We also describe the hysteresis observed in high transmission properties of PMMABA/E7 and a memory effect in PMMABA/E8 during electrooptic switching. The possible mechanisms of both phenomena are discussed in terms of an interfacial interaction between the polymer matrix and LC molecules.

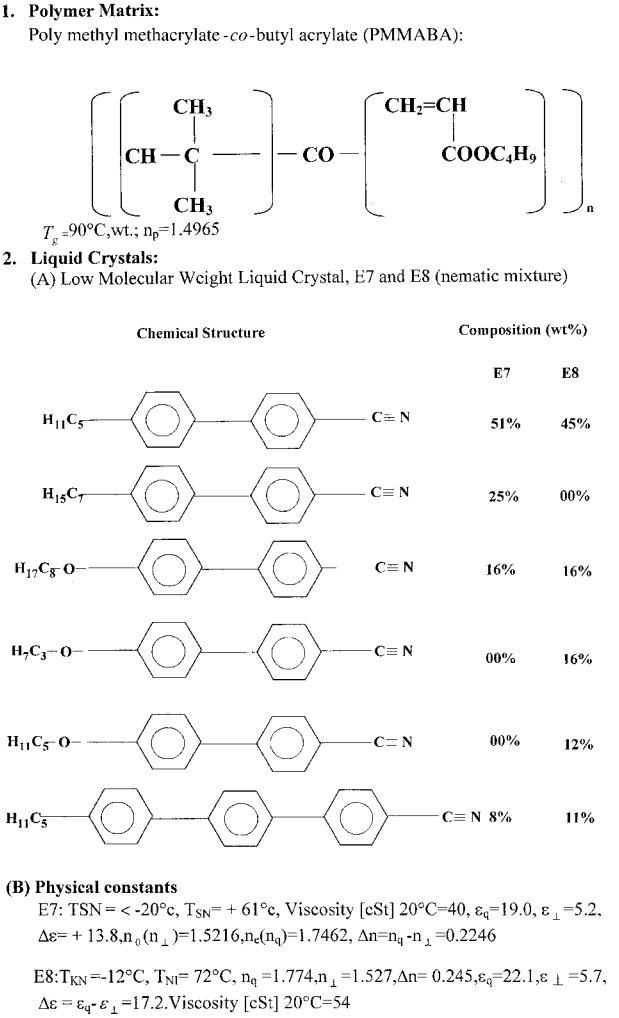


**Figure 1** Chemical structures and physical properties of the polymer matrix PMMABA and nematic LCs E7 and E8.

## EXPERIMENTAL

### Materials

The nematic LCs (E7 and E8; E. Merck, Darmstadt, Germany) used in this study were eutectic mixtures of a number of cynophenyl derivatives with positive dielectric anisotropy. The polymer mixture was a copolymer of poly(methyl methacrylate) and butyl acrylate (PMMABA; Degussa Corp., Düsseldorf, Germany). The chemical structures and physical properties of these constituents for the PDLC films are given in Figure 1.

### Preparation of the PDLC films

The PDLC films were prepared by a solvent-induced phase-separation technique. PDLC films of different polymer/LC compositions (wt/wt %) were prepared from a homogeneous solution of an appropriate amount of E7 or E8 and a polymer (PMMABA) in chloroform (analytical-reagent grade), which was spread over indium tin oxide (ITO) coated glass as a substrate at room temperature (28°C). The two PDLC composite films were prepared simultaneously. The solvent evaporation rate during film preparation for both systems (PMMABA/E7 and PMMABA/E8) was controlled by the regulation of the pressure in the solvent evaporation chamber with a needle valve and a vacuum pump to dominantly produce LC-induced aggregation structures of the matrix polymer. The sample PDLC films were sandwiched between two ITO-coated glass plates (200 Ω/□) with dimensions of 6 mm × 6 mm, which were separated by a poly(ethylene terephthalate) film spacer of various electrooptic measurements that for both PDLC films was 10 ± 2 μm.

### Electrooptic measurements

To evaluate the electrooptic properties of the PDLC composite films, light transmission changes upon the

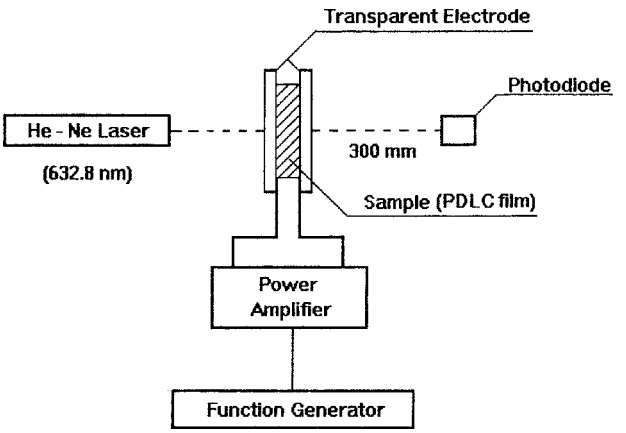


**Figure 2** Schematic illustration of the measuring system used for the electrooptic properties of the composite system.

application of an alternating-current (ac) electric field were studied. The experimental system for these studies is shown schematically in Figure 2. The collimated beam of a model 105 P polarized He–Ne laser (wavelength = 632.8 nm with 5 mW of power; Photochemical, Inc., Toronto, Canada) was used as an incident light source. The transmitted light intensity without any polarizer was measured under the modulation of an ac electric field in normal transmission geometry with a photodiode (Jain-Laser Tech, Mumbai, Maharashtra, India). An ac electric field was provided by the amplification of the signal (50-, 100-, 500-, and 1-kHz square waves) from a function generator with a power amplifier and its application to the conducting electrodes to drive the shutter. The response of the photodiode was monitored with a digital storage oscilloscope (TDS 430A, Tektronix; 400 MHz, Beaverton, OR); for response-time measurements, the PDLC films were driven by a sinusoidal voltage with a driving frequency of 1 kHz with a nearly 1-s pulse. The distance between the cell and photodiode was 3000 mm.

### Morphology

The morphologies of the PDLC composite films were studied with a Cambridge Stereoscan 150 scanning electron microscope (Cambridge Instruments (LEO), Cambridge, UK). For structural studies, the LC was removed from the films by the solvent-extraction method at room temperature (28°C), and then the films were dried overnight under vacuum. The dried films were fractured in liquid nitrogen. A thin conducting layer of gold was vacuum-sputtered onto the structure before it was viewed under the scanning electron microscope. Also, a crossed polarized microscope (AXIO-LAB-100 trinocular research microscope, Carl Zeiss, London, UK) was used to record the director configuration behavior of the LC microdomains in the composite films.

### Fourier transform infrared (FTIR) measurements

The phase mixing at the polymer–LC interface was studied with an FTIR spectrometer (Paragon 500, PerkinElmer, MA) at a resolution of 4 $cm^{-1}$. The internal reflection attachment, equipped with a KRS-5 crystal (incident angle = 45°), was used for attenuated total reflection (ATR) measurements. To evaluate the amount of LC penetration into the matrix polymer with ATR, the polymer film surface was first placed in contact with the LC for 1 h, and then the LC was rinsed with methanol. Similarly, to observe the effect of temperature on the penetration of the LC into the polymer matrix, the polymer was placed in contact with the LC at room temperature (28°C) and above the clearing temperature of the LC (E7, 61°C; E8, 72°C).

### Thermal analysis

The different thermal transitions of the polymer LCs and polymer/LC composites were measured with a PerkinElmer DSC-7 differential scanning calorimeter. The differential scanning calorimetry (DSC) scanning rate was 5°C/min under a dry nitrogen atmosphere.

## RESULTS AND DISCUSSION

### Effects of the PDLC film parameters

Figure 3 shows the off-state and on-state transmissions of PMMABA films of various E7 and E8 con-

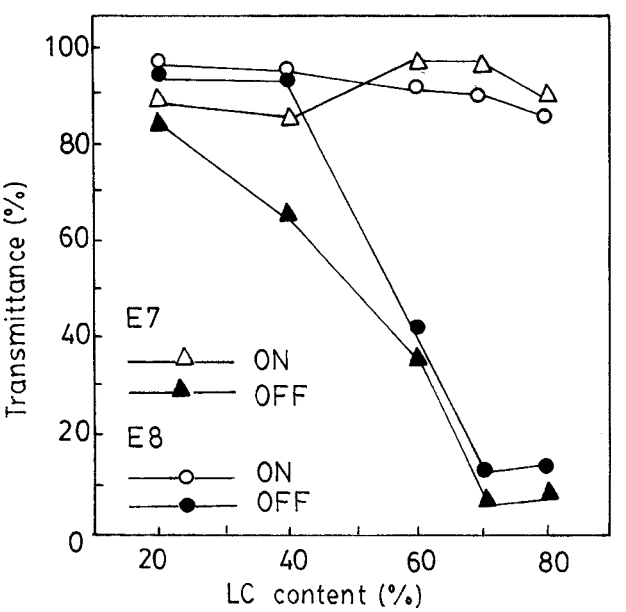


**Figure 3** Optical contrast of unpowered and powered PMMABA/LC composite films versus the LC content (the power on corresponds to 1 kHz, 200 Vp-p, and 28°C).

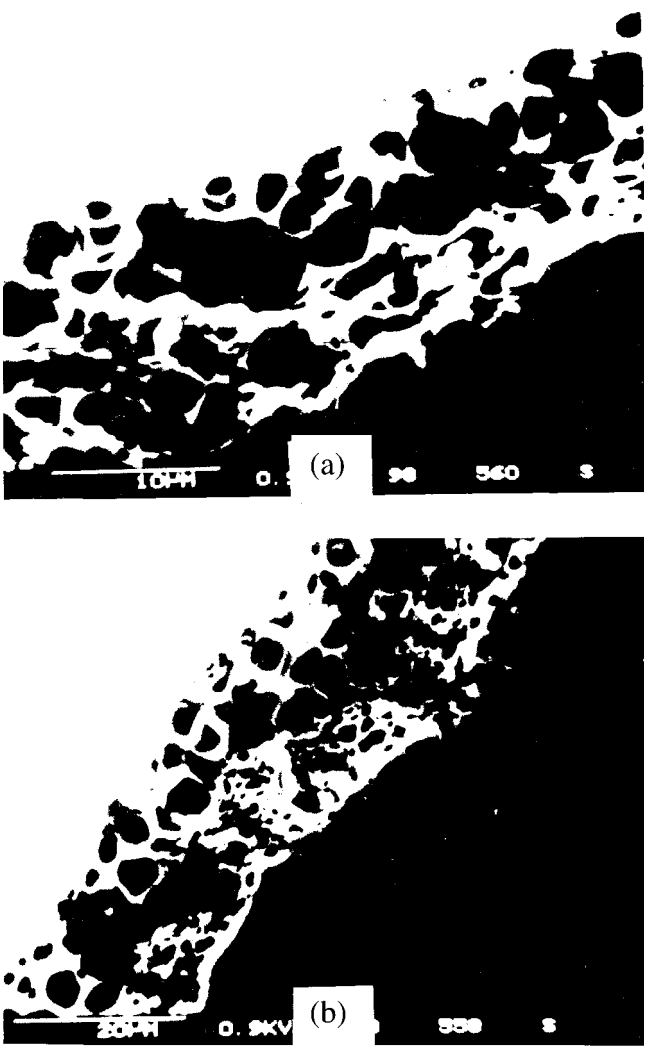


**Figure 4** Scanning electron micrographs of cryogenically fractured films: (a) PMMABA/E7 (30/70 w/w) and (b) PMMABA/E8 (30/70 w/w) composite films.

tents measured at 1 kHz, 200 Vp-p, and 28°C. The main consideration of these experiments was the necessity of optimization of these PDLC films for the LC loading and film thickness from the point of view of maximum optical contrast. In the absence of an ac electric field, strong light intensity contrast (defined as the maximum difference between the magnitudes of transmittance with on and off ac electric fields) appeared in the range of 70–80% (w/w) for both E7 and E8 in the composite films. Similarly, under the general conditions of the experimental setup, the intensity of the light sources, and the magnitudes of the applied voltage, both composite films with a thickness of about 20 ± 2 μm gave significant optical contrast, and thus further experiments were performed with films of this thickness at a fixed composition of 30/70 wt %.

### Microscopic structure of the polymer/LC composite films

Figure 4 shows scanning electron micrographs obtained from cryogenically fractured cross sections of PMMABA/E7 and PMMABA/E8 composite films (30/70 wt %) after the removal of the LC. It was observed in both cases that with low LC loadings, spherical droplets interconnected to form larger ones. Here the droplet size ranged from submicrometers to several micrometers. As the LC content ultimately increased to 70 wt % in the films, the micrograph shows larger elongated LC cavities interconnected in three dimensions as a continuous phase and separated by thin PMMABA matrix polymer walls forming a three-dimensional spongy network. These droplet cavities in general were very large spheroids, with the major axis lying parallel to the film base. Because in this case the films were prepared with solvent-induced phase-separation techniques, the small LC domains were formed upon solvent evaporation, and this was followed by coalescence of these small domains to form larger ones. The process eventually led to the formation of interconnected LC channels when the LC loading was high enough.

Figure 5 shows a polarized optical micrograph of the PMMABA/E7 composite system viewed from the top of the film surface. The focused view of the LC microdomain under crossed polarizes shows that the large domains were in a bipolar configuration. Such a polar orientation is predominantly observed in films with continuous, interconnected channels in which LC molecules are anchored tangentially to the matrix polymer wall. A similar director configura-

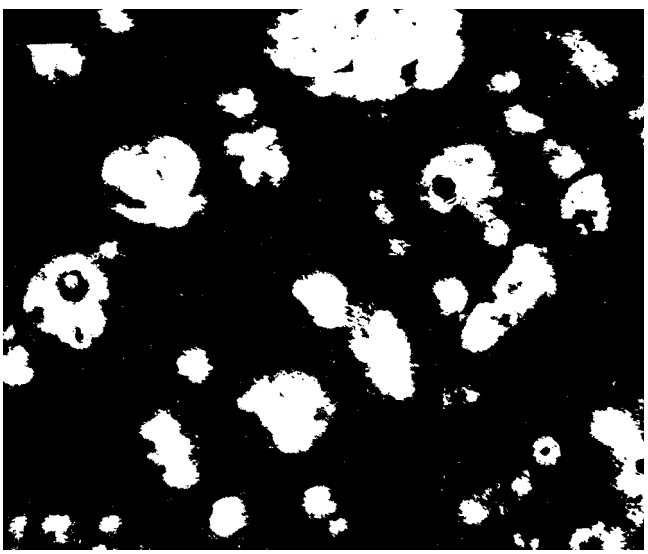

**Figure 5** Unpowered photomicrograph of the director configuration of E7 droplets in a PMMABA/E7 (30/70 w/w) composite film observed under a microscope between crossed polarizers.

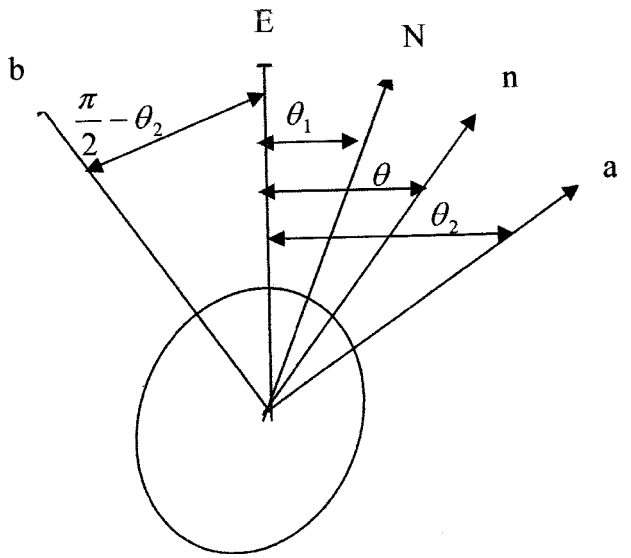


**Figure 6** Illustration of the arbitrarily oriented droplet director in an elongated droplet (Wu et al.'s model).

tion was also observed in the PMMABA/E8 composite system.

The observed morphology indicates that both composite systems, PMMABA/E7 and PMMABA/E8, can be taken as binary dielectrics with the polymer and LC as the components. This structural heterogeneity corresponds to a basic sources of optical heterogeneity for the composites in the off-state external field.

### Voltage dependence of the transmittance and response time

On the basis of Wu et al.'s model,[33] the application of an electric field ($E$) reorients the elongated droplet nematic director ($n$) to its equilibrium orientation ($N$; Fig. 6). If $\theta_1$ is the angle between the direction of $N$ and $E$, Wu et al.'s model describes $\theta_1$ as follows:

$$\theta_1 = \frac{1}{2}\tan^{-1}\left(\frac{\sin 2\theta_2}{A+\cos 2\theta_2}\right) \tag{1}$$

$\theta_1$ and $\theta_2$ are defined in Figure 6, and $A = \Delta\varepsilon a^2\varepsilon^2/K(l^2 - 1)$, where $\Delta\varepsilon$ is the dielectric anisotropy, $K$ is the effective elastic constant and $l = (a/b)$, where $a$ and $b$ are the lengths of the semi-major and semiminor axis, respectively. The equation indicates that $N$ gradually approaches the direction of $E$ with increasing field strength in an elongated LC droplet, provided that $\Delta\varepsilon$ is positive. In such a situation, the LC molecules in a PDLC film will align with their long molecular axis parallel to the applied field with a minimum energy level.

Thus, according to the model, the switching voltage [i.e., threshold voltage ($V_{th}$)] for the director reorientation in droplets with a bipolar configuration, which results in a variation of the optical transmission of the PDLC system, is determined by the balance between the elastic force, surface interaction, and applied electric force and is estimated as follows:

$$V_{th} = \frac{d}{3a}\left(\frac{P_P}{P_{LC}}+2\right)\left(\frac{K(\ell^2-1)^{\frac{1}{2}}}{\Delta\varepsilon}\right) \tag{2}$$

where $d$ is the cell thickness; $P_P$ and $P_{LC}$ are the resistivities of the polymer and LC, respectively; $\ell = a/b$, where $a$ and $b$ are the lengths of the semimajor and semiminor axes of the LC droplet, respectively; $K$ is the elastic constant; and $\Delta\varepsilon$ is the dielectric anisotropy of the LC.

To characterize the time-dependent transmittance response in both systems (PMMABA/E7 and PMMABA/E8), a sinusoidal voltage at a 1-kHz frequency was supplied to composite films for a period of 60 ms. Figure 7 shows the time-dependent transmittance variations with the voltage at room temperature for the PMMABA/E7 composite. At a low applied voltage, the transmittance increased asymptotically with time, whereas at a high voltage, it increased rapidly to much higher saturation values. A similar trend was also observed for the PMMABA/E8 composite system.

Figure 8 shows the transmittance as a function of the applied voltage at 1 kHz. The transmittance in PMMABA/E7 almost was unchanged with the applied voltage up to 10–20 Vp-p, whereas in the case of the PMMABA/E8 composite, this threshold

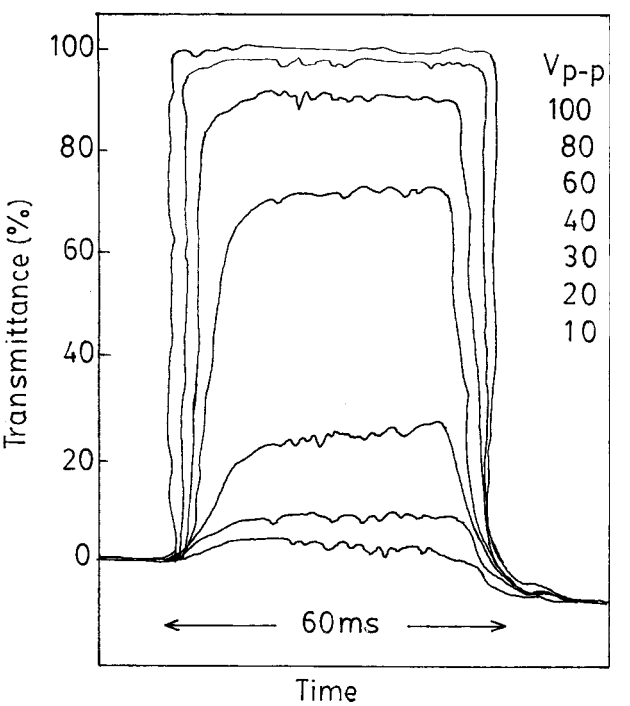


**Figure 7** Time-dependent transmittance for a PMMABA/E7 composite film at 1 kHz, 10–100 Vp-p, and 28°C.

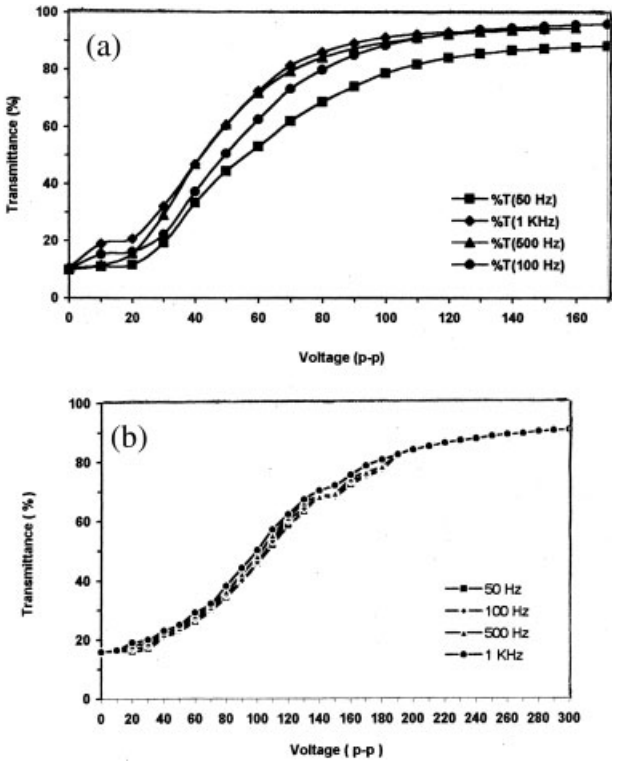


**Figure 8** Applied voltage dependence of the light transmittance for (a) PMMABA/E7 and (b) PMMABA/E8 (30/70 w/w) composite films at different frequencies.

electric voltage was at 30–35 Vp-p. The comparatively high value in the latter case was due to the strong interfacial interaction between PMMABA and E8. The lower glass-transition temperature ($T_g$) of PMMABA/E7 versus that of the PMMABA/E8 composite indicates the higher order modification of surface interaction through enhanced miscibility, resulting in less anchoring energy of LC (E7) molecules on the matrix polymer wall[34] (Fig. 9). Additionally, with the smaller dimensions of E8 domains (3–4 μm) in comparison with E7 (5–7 μm) in the composite, more E8 molecules interacted with the polymer wall, and a stronger external field was required to overcome the interfacial interactions in the PMMABA/E8 composite and to align them along the electric field. This contributed to higher $V_{th}$ values in E8 composites than E7. Also, the droplet elongation deformation in the case of PMMABA/E7 (Fig. 4) was more parallel to the electric field direction, and the elastic energy was smaller; this also physically contributed to the lower $V_{th}$ value of the PMMABA/E7 composite.

Figure 10 shows the increasing and decreasing process of the applied voltage dependence of the transmittance for the PMMABA/E7 composite film as a function of the switching frequency. Here the amplitude of an applied voltage was modulated linearly. The PMMABA/E7 films exhibited electrooptic switching hystereses. The degree of the hysteresis was apparent in all cases of switching frequency from 50 HZ to 1 kHz. The basic reason for hysteresis in PDLC films has been the topic of several discussions.[35–37] However, the phenomenon may be related to the mechanism of orientation of the LC droplet director,[38] which may depend on the LC/polymer compatibility-induced interfacial polarization process, which ultimately influences the distribution of the relaxation time.[30] As mentioned previously, the possible compatibility of PMMABA and E7 in the composite film was confirmed by the observed lowering of $T_g$ of PMMABA in the PMMABA/E7 composite (Fig. 9). The phase-mixing behavior at the PMMABA/E7 composite interface was examined with measurements of the FTIR spectra. The absorption peak at 2226.4 $cm^{-1}$, corresponding to C≡N stretching, was observed even after E7 was removed with methanol from the film surface, and this indicated the PMMABA/E7 phase mixing at the composite interface. The intensity of this C≡N stretching band increased with an increasing E7-contact tem-

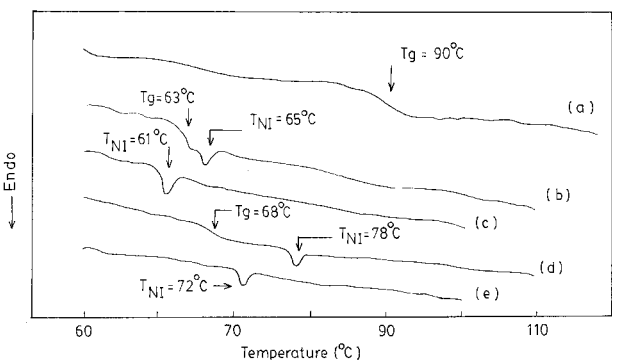


**Figure 9** DSC thermograms of (a) pure PMMABA, (b) PMMABA/E7 (50/50 w/w) (c) pure E7, (d) PMMABA/E8 (50/50 w/w), and (e) pure E8 LC.

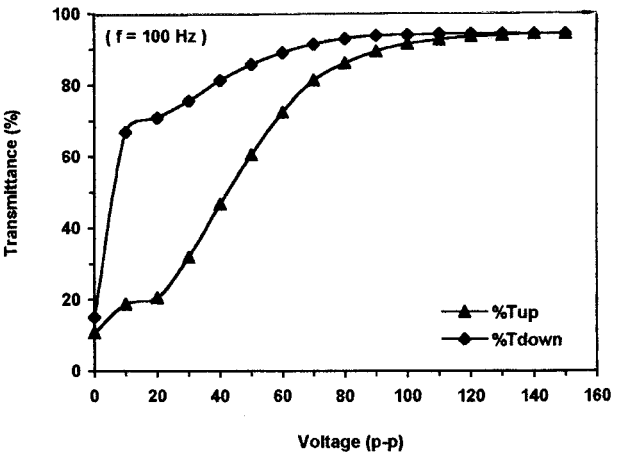


**Figure 10** Applied voltage dependence of the light transmission with hysteresis for a PMMABA/E7 (30/70 w/w) composite film at a fixed switching frequency of 100 Hz.

perature. This clearly suggests that E7 penetrated the PMMABA film, and the magnitude of the penetration increased with increasing temperature (Fig. 11). Furthermore, it was observed that this 2226.4-$cm^{-1}$ band in the PMMABA/E7 composite exhibited an absorption intensity gain in the electric-field on state in comparison to the electric-field off state. These experimental observations support the electric-field-induced phase mixing at the PMMABA/E7 interface. In such a situation of endothermic structural changes in the on state of an electric field, the recovery process to the original off-state dielectric structure of a composite takes longer. Hence, it is suggested that in this case, the phase mixing at the PMMABA/E7 interface, induced upon the application of an ac electric field, may have been a mechanism of electrooptic switching hysteresis.

In the case of PMMABA/E8, the composite films showed higher transmittance (Fig. 12) even after the voltage application (memory state) than those in their initial off state. Similar to PMMABA/E7, these composites also exhibited phase-mixing behavior at the interface and the lowering of $T_g$ of PMMABA. In this case (PMMABA/E7), an absorption peak at 2225.9 $cm^{-1}$ corresponding to C≡N stretching of E7 was also observed even after the removal of E7 from the composite film surface. In such a morphological situation, the on-state-induced dielectric loss energy in the composite results in thermodynamic changes, which hinder the recovery process to the original structure in the off state. These structural changes induce enhanced disorder of the bipolar orientation, introducing longer relaxation times and thus ultimately creating memory states. In a memory state, it can be assumed that the LCs in the PDLC composite still tend to maintain their alignment partially in the direction of the electric field in the off state. In this case, the memory state could be erased by the heating of the composite films up to the clearing temperature of LC, that is, 72°C for E8.

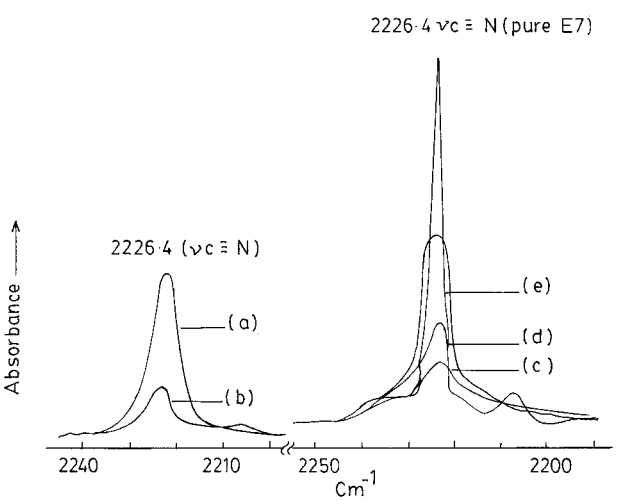


**Figure 11** FTIR–ATR spectra of the C≡N stretching vibration for a composite film surface (a) after surface contact with E7 at room temperature (28°C) and (b) after the removal of E7 from the composite film surface by solvent washing and spectra of composite films after the contact of the films with E7 at contact temperatures of (c) 28, (d) 110, and (e) 120°C.

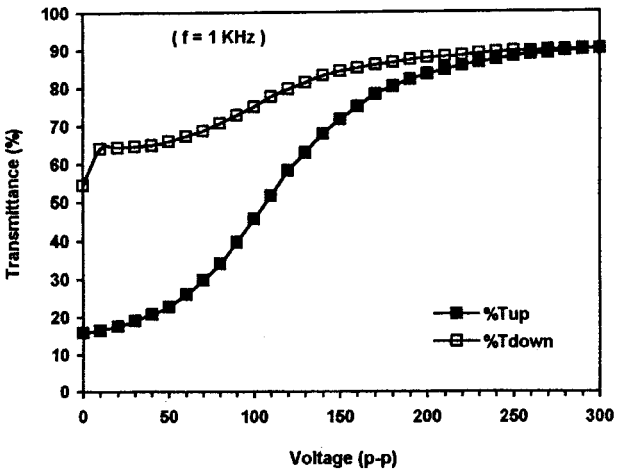


**Figure 12** Applied voltage dependence of the light transmittance with memory for PMMABA/E7 at a fixed switching frequency of 1 kHz.

For an elongated droplet of aspect ratio $\ell$, the rise time ($T_R$), which is defined as the time required for transmittance changes from 10 to 90% upon the powering of the film, and the decay time ($T_D$), which is measured when the applied voltage is turned off, can be calculated with eqs. (3) and (4), respectively:[33]

$$\frac{1}{T_R} = \frac{1}{\eta}\frac{q\varepsilon_o \Delta\varepsilon V^2}{d^2(P_P/P_{LC}+2)^2} + \frac{K(\ell^2-1)}{\eta a^2} \tag{3}$$

$$\frac{1}{T_D} = \frac{\eta a^2}{K(\ell^2-1)} \tag{4}$$

where $\eta$, $\varepsilon_o$, and $V$ represent the rotational viscosity of the LC, vacuum permittivity, and applied voltage, respectively, and other symbols bear the same meanings given earlier. An analysis of eqs. (3) and (4) indicates that $T_R$ is predominantly a function of the applied voltage, whereas $T_D$ depends on the LC domain size and shape. In this case, the PMMABA/E7 composite system showed smaller $T_R$ [Fig. 13(a)] than the composites with E8. This may be due to the larger E7 domains resulting in a smaller interfacial area than E8. However, with increasing LC loading, in both cases a marginal decrease in $T_R$ was observed.

Figure 13(b) shows $T_D$ as a function of the applied voltage for these composites. $T_D$ of these films

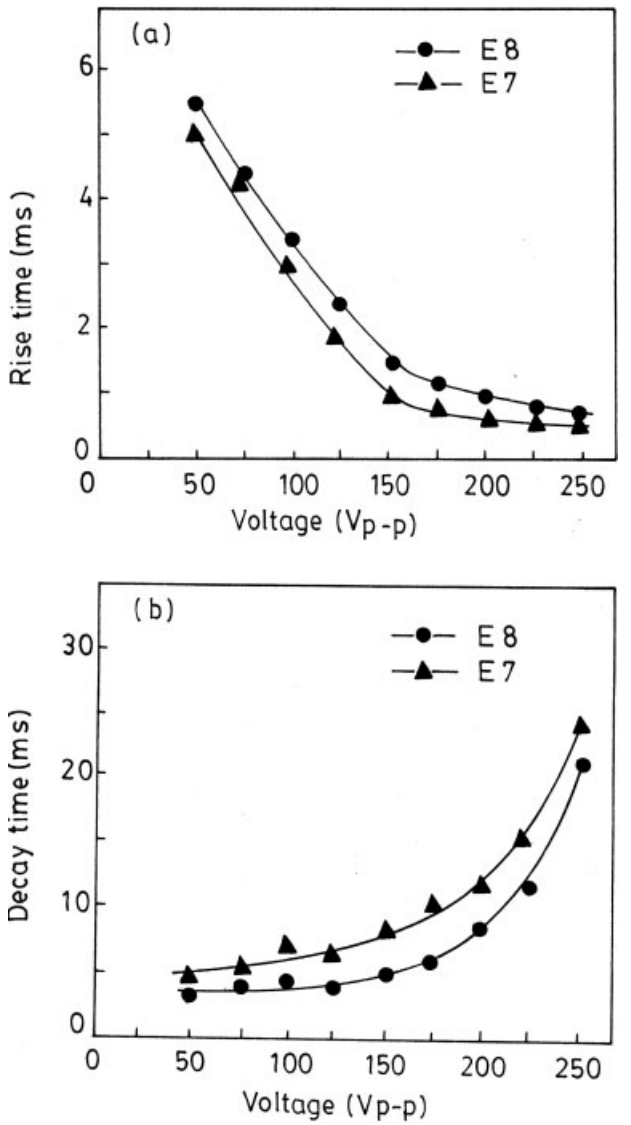


**Figure 13** $T_R$ and $T_D$ versus the applied voltage for (a) PMMABA/E7 and (b) PMMABA/E8 composite films at a frequency of 1 kHz and 28°C.

showed the opposite tendency of $T_R$, as it was apparently independent of the applied voltage. From the figure, it follows that the PMMABA/E8 composite took less time to decay than PMMABA/E7. This may be primarily due to the smaller dimensions of the E8 domain (LC) morphology in the composite, which resulted in stronger LC–polymer interfacial interactions, which in fact facilitated the faster randomization of the nematic directors. However, in both composite systems, $T_D$ increased with increasing applied voltage. This may be due to the higher order of alignment of the LC molecules and the bipolar axis along the applied electric field direction. This requires much greater distortion of the director upon field removal and in turn a greater restoration energy, resulting in an overall slow relaxation process at higher voltages.

### Temperature dependence of the transmittance and response time

In practical applications, devices based on PDLC films with both high on-state transmittance and strong off-state attenuation are often subjected to a wide range of operating temperatures. It is thus important to study the temperature dependence of these electrooptic responses. It is known that $K$ and $\Delta\varepsilon$ of typical nematic LCs are strongly dependent on the temperature. According to the mean field theory proposed by Maier and Saup,[39] $K$ is proportional to the square of order parameter $S$ and $\Delta\varepsilon$ is proportional to $S$. Here it is assumed that the ratio of the LC conductivity to the conductivity of the matrix polymer is independent of the temperature. Furthermore, for many nematic LCs, $S$ is approximately proportional to $(T/T_{NI})^{-r}$, where $r$ is on the order of 0.08, $T$ is the temperature, and $T_{NI}$ is the nematic–isotropic transition temperature.[40] Thus, the theory leads to the $(V_{th})(T)^{0.4}$ product being approximately a constant value.[39] In this case, the variation of the observed $V_{th}$ values with respect to the temperature is presented in Figure 14, and it follows the relation approximately.

The transmittance of both the PMMAMA/E7 and PMMABA/E8 composite in the absence of high volt-

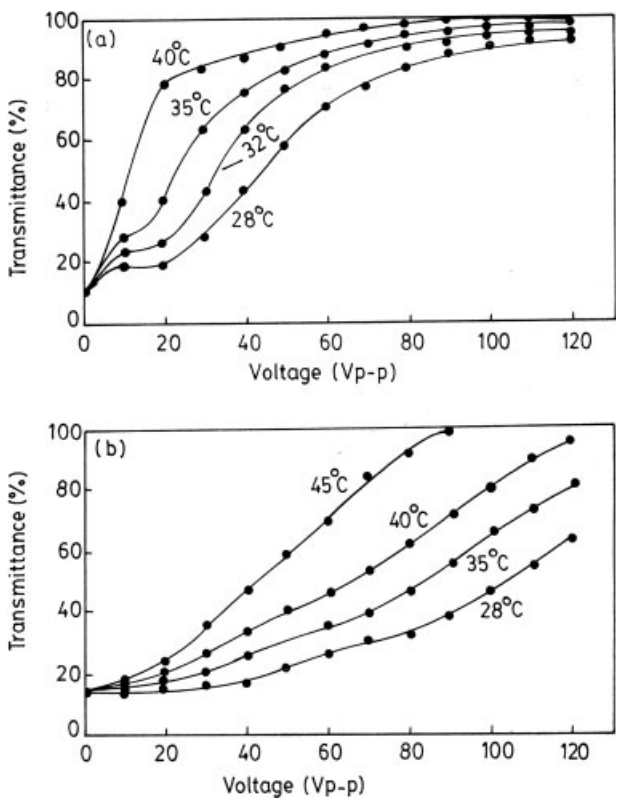


**Figure 14** Variation of the observed $V_{th}$ values with respect to the temperature of unpowered films of (a) PMMABA/E7 and (b) PMMABA/E8.

age increased with increasing temperature, particularly at high temperatures (Fig. 15). This increase in transmittances was caused by the decrease in the birefringence ($\Delta n = n_e - n_o$, where $n_e$ is the extraordinary refractive index and $n_o$ is the ordinary refractive index) of the LCs[41] and their increased solubility in the polymer matrix.[42] $n_e$ decreased and $n_o$ increased with the increase in temperature, and this resulted in the overall decreases in $\Delta n$ with the temperature:[43,44]

$$\Delta n \propto \left(1 - \frac{0.98}{T_{NI}}\right)^{0.22} \tag{5}$$

Also, in agreement with the mean field theory,[39] $A^2 = \varepsilon a^2 E^2 / K(l^2 - 1)$ is approximately proportional to

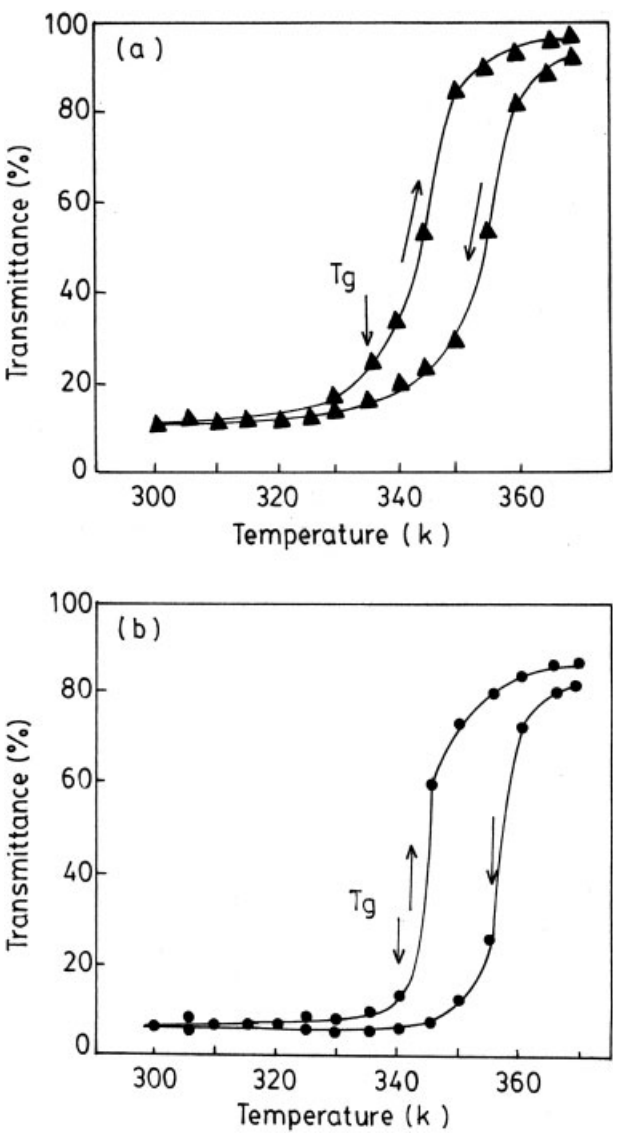


**Figure 15** Variation of the transmittance with respect to the temperature of unpowered composite films of (a) PMMABA/E7 and (b) PMMABA/E8.

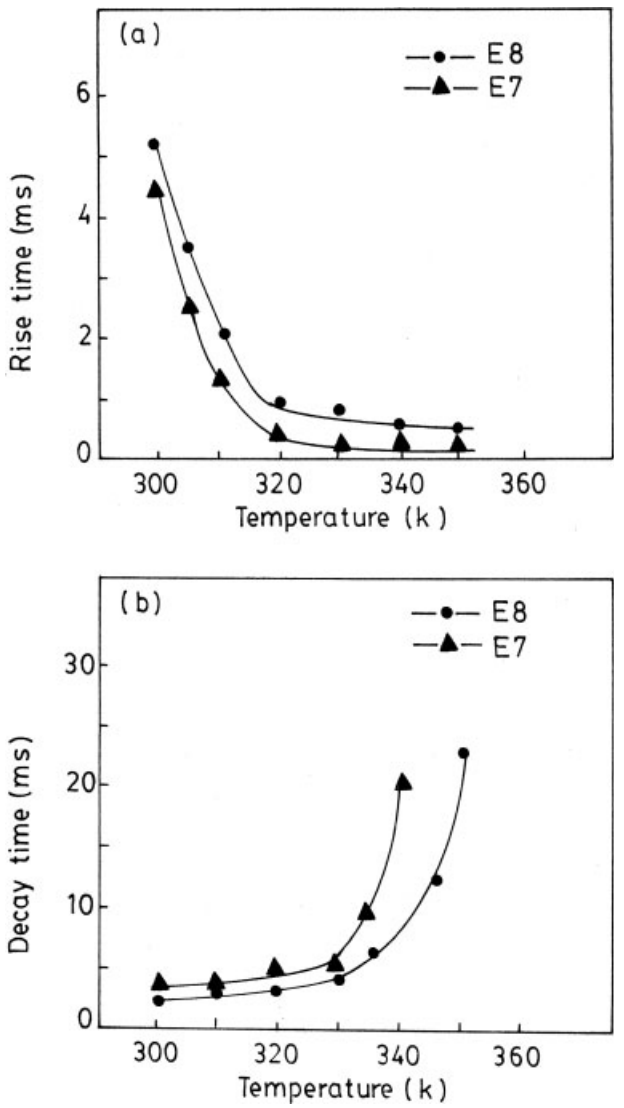


**Figure 16** $T_R$ and $T_D$ versus the temperature for (a) PMMABA/E7 and (b) PMMABA/E8 composite films.

$(T/T_{NI})^{0.7}$, which in fact reduces $\theta_1$, the angle between the direction of $N$ and $E$ in Wu et al.'s model[33] (Fig. 6), at a higher temperature and a low applied voltage. The maximum transmission is thus shifted to the higher temperatures predominantly because of the decreased mismatching of refractivity with increased temperatures.

$T_R$ (10–90%) and $T_D$ (90–10%) of the PMMABA/E7 and PMMABA/E8 composites at various ambient temperatures are shown in Figure 16. According to Wu et al.'s model,[33] for large voltages, $T_R$ and $T_D$ are approximately proportional to $\eta/\Delta\varepsilon$ and $\eta/K$, respectively. Furthermore, as shown by the analysis of Wu et al.'s model, the dependences of $T_R$ and $T_D$ on $V$ and $T$ can be given as $T_R V^2 T^{1.5}$ = constant and $T_D T^{0.8}$ = constant, respectively. The results given in Figure 16 follow this relationship approximately. In this case, $T_R$ decreased with increasing voltage as

well as temperature. This may be due to the decrease in $\eta$ affecting the interfacial interaction between the polymer wall and LC molecules. $T_D$ depends on a time constant with $V = 0$. However, as $\eta$ and $K$ both decrease with increasing temperature, the observed increase in $T_D$ with increasing temperature may be understood in terms of enhanced thermal molecular motion of the matrix polymer chain, which delays the reorientation of LC directors to a random orientation state.

### Frequency dependence of the transmittance and response time

Figure 8 shows that for both composites, PMMABA/E7 and PMMABA/E8, the transmission at a fixed applied voltage increased gradually with an increase in the frequency with the experimental conditions of 200 Vp-p and 28°C. When the experiments were performed at low frequencies (<50 Hz), at very low frequencies, the transmittance oscillated with twice the electric frequency as the LC followed the driving voltage, whereas at high enough frequencies, the transmittances did not follow the electric oscillation, and eventually the oscillation damped out. The response of the LC no longer followed the change in the electric polarity.[36,42,45–48] For a series-connected dielectric composite model that is quite analogous to the present polymer/LC composite films, the applied electric field is not totally imposed on the LC phase but depends on the magnitude of the dielectric constants and the conductivity of the matrix polymer and LC.[17,37,38] This partition of the external electric field to LC is given by eq. (5):

$$\frac{E_{LC}}{E_P} = \frac{|\varepsilon_P^*|}{|\varepsilon_{LC}^*|} = \left[\frac{(\omega^2\varepsilon_P^2 + \sigma_P^2)}{(\omega^2\varepsilon_{LC}^2 + \sigma_{LC})}\right]^{\frac{1}{2}} \quad (6)$$

where $E$, $\varepsilon^*$ and $\varepsilon$, $\sigma$, and $\omega$ represent the applied external electric field, the complex and in-phase components, the conductivity, and the angular frequency, respectively. The equation clearly states that at low frequencies, the ratio of the local electric fields in the LC and polymer ($E_{LC}/E_P$) is inversely proportional to the conductivity ratio ($\sigma_P/\sigma_{LC}$), whereas at high frequencies, it is inversely proportional to the ratio of the dielectric constants of the two phases ($\varepsilon_P/\varepsilon_{LC}$). $E_{LC}/E_P$ is generally larger than $\sigma_P/\sigma_{LC}$; interfacial polarization is induced at low frequencies, and consequently, the magnitude of $E_{LC}/E_P$ decreases in the frequency range near and below the relaxation frequency of the interfacial polarization.[26,45] In such a situation, the local field of the LC ($E_{LC}$) rapidly decreases with a decrease in frequency. However, at high frequencies, because of a high local field imposed on the LC, the time is insufficient to allow the relaxation of the LC nematic director to an unaligned position and thus results in high transmission, as observed in Figure 8.

Figure 17 shows the measured optical $T_R$ and $T_D$ values as a function of the frequency. Because the magnitude of the effective electric field in the LC phase ($E_{LC}$) decreases with a decrease in the frequency of an applied electric field [eq. (5)], $T_R$ is expected to decrease with increasing frequency,[48,49] and this is consistent with our experimental results. The two composite films agreed with each other with respect to $T_R$. However, as mentioned earlier, their $T_D$ behaviors were completely different. The PMMABA/E7 composite film exhibited a fast decay, whereas PMMABA/E8 showed a slow decay. Such behavior may be attributed to the local molecular

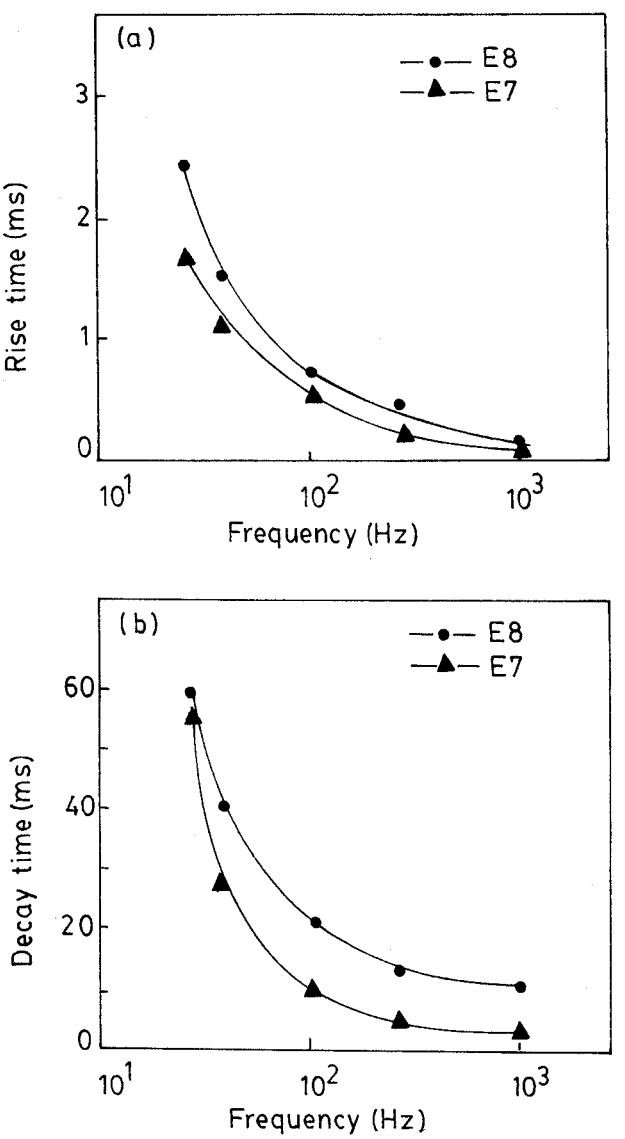


**Figure 17** $T_R$ and $T_D$ versus the applied frequency for (a) PMMABA/E7 and (b) PMMABA/E8 composite films at 200 Vp-p and 28°C.

motion of the matrix (PMMABA) induced by polymer–LC interactions.

## CONCLUSIONS

We studied the electrooptic properties as a function of the voltage, temperature, and frequency of PDLC films composed of nematic LCs (E7 and E8) dispersed as droplets in a PMMABA matrix polymer. The LC domains for E7 were larger and more elongated (electric field direction) than those for E8 in composites. The composite films studied here were also characterized for their composite structure. Both LCs, E7 and E8, lowered $T_g$ of the PMMABA matrix. It has been postulated that the higher the solubility is, the lower $T_g$ is and thus the lower the surface interactions are between the LC and the matrix polymer in composites. In such a case, a smaller electric field becomes necessary to overcome the interfacial interactions, and this consequently lowers the $V_{th}$ value required for the orientation of nematic directors in a bipolar configuration. The PDLC film containing the LC E7 showed lower $V_{th}$, lower $T_R$ and $T_D$, and higher transmittance. Such electrooptic behavior was due primarily to the E7 droplet morphology in comparison with E8 in the composite and the increased solubility of E7 in the PMMABA polymer matrix. The electrooptic switching hysteresis/memory observed in the increasing and decreasing processes of an applied electric voltage depended on the compatibility between the polymer and LC, which was induced by the application of an electric field.

## References


1. Young, W.; Bahadur, B.; Lewis, D.; Wan, K. SID Dig Tech Pap 1994, 25, 611.
2. Drzaic, P. S. Mol Cryst Liq Cryst 1991, 198, 61.
3. Doane, J. W.; West, J. L.; Whithead, J. B.; Fredly, D. S. SID Dig Tech Pap 1990, 21, 224.
4. West, J. L.; Ondrise, R.-J.; Crawford, R. J. J Appl Phys 1991, 70, 3785.
5. Drzaic, P. S.; Gonzales, A. M.; Jones, P.; Montoya, W. SID Dig Tech Pap 1992, 23, 571.
6. West, J. L. In Technological Applications of Dispersions; Mckay, R. B., Ed.; Marcel Dekker: New York, 1994; Chapter 10.
7. Coates, D. Displays 1993, 14, 94.
8. Kinugasa, N.; Yano, Y.; Nagyama, H.; Yosida, H.; Watanabe. SID Dig Tech Pap 1991, 22, 598.
9. Wakabayashi, T.; Iida, S.; Gunjima, T. SID Dig Tech Pap 1993, 24, 869.
10. Jons, P.; Montoya, W.; Garza, G.; Engler, S. SID Dig Tech Pap 1992, 23, 762.
11. Tomita, A. SID Dig Tech Pap 1993, 24, 865.
12. Takizawa, K.; Kikuchi, H.; Fujikake, H. SID Dig Tech Pap 1991, 22, 250.
13. Sutherland, R. L.; Natrajan, L. V.; Tondiglia, V. P.; Bunning, T. J. Chem Mater 1993, 5, 1533.
14. Tanaka, K.; Katoh, K.; Tsura, S.; Saki, T. J SID 1994, 2, 37.
15. Lee, S. N.; Sprunt, S.; Chien, L. C. Liq Cryst 2001, 28, 637.
16. Senyuk, I.; Smalyukh, I. I.; Lavrentovich, O. D. Opt Lett 2005, 30, 249.
17. West, J. L.; Zhang, G.; Glushchenko, A. SID Dig 2003, 55, 1.
18. West, J. L.; Zhang, K.; Zhang, M.; Buyuktanir, E.; Glushchenko, A. Proc SPIE 2005, 59360 L, 5936.
19. Fulghum, J. E.; Su, L.; Artyushkova, K.; West, J. L.; Reznikov, R. Mol Cryst Liq Cryst 2004, 412, 361.
20. Zhang, G.; West, J. L.; Glushchenko, A.; Smalyukh, I. I.; Laverentovich, O. Proc SID 2005; p 5.
21. West, J. L.; Zhang, K.; Zhang, M.; Aoki, T.; Glushchenko, A. Proc SPIE 2005, 10, 5741.
22. Golovin, A. B.; Shiyanovskii, S. V.; Laverentovich, O. D. Appl Phys 2003, 83, 3864.
23. Buyuktanir, E. A.; Glushchenko, A.; Wall, B.; West, J. L. Proc SID 2005, p 1778.
24. Yang, D. K.; Crooker, P. P. Liq Cryst 1991, 9, 245.
25. Miyamoto, A.; Kikuchi, H.; Morimura, Y.; Kajiyama, T. New Polym Mater 1990, 2, 27.
26. Miyamoto, A.; Kikuchi, H.; Kobayashi, S.; Morimura, Y.; Kajiyama, T. Macromolecules 1991, 24, 3915.
27. Kajiyama, T.; Kikuchi, H. J Chem Soc Jpn Chem Ind Chem 1992, 10, 1019.
28. Kajiyama, T.; Park, K.; Usui, H.; Kikuchi, H.; Takahara, A. Proc SPIE 1993, 122, 1911.
29. Park, K.; Kikuchi, H.; Kajiyama, T. Polym J 1994, 26, 895.
30. Drzaic, P. S. Liquid Crystal Dispersion; World Scientific: Singapore, 1995.
31. Kalkar, A. K.; Kunte, V. V.; Deshpande, A. A. J Appl Polym Sci 1999, 74, 3485.
32. Kalkar, A. K.; Kunte, V. V. Mol Cryst Liq Cryst 2002, 383, 1.
33. Wu, B. G.; Erdmann, J. H.; Doane, J. W. Liq Cryst 1989, 5, 1453.
34. Zumer, S.; Doane, J. W. Phys Rev A 1986, 34, 3373.
35. Drzaic, P. S. Liq Cryst 1988, 3, 1543.
36. Jain, S. C.; Raut, D. K. J Appl Phys 1991, 70, 6988.
37. Reamey, R. H.; Montoya, W.; Wong, A. Proc SPIE 1992, 2, 1665.
38. Kelly, J. R.; Wu, W.; Palffy-Muhoray, P. Mol Cryst Liq Cryst 1994, 243, 11.
39. Maier, W.; Saupe, A. Z Naturforsch A 1960, 15, 827.
40. Yakhmi, J. V.; Kelmer, Y. K.; Shukla, R. P.; Manohar, C. Mol Cryst Liq Cryst 1979, 53, 55.
41. Vaz, N. A.; Montgomery, G., Jr. J Appl Phys 1987, 62, 3161.
42. Miyamoto, A.; Kikuchi, H.; Morimura, Y.; Kajiyama, T. New Polym Mater 1990, 2, 1.
43. Pohl, L.; Merck, E. Liquid Crystal—Applications and Uses; World Scientific: Singapore, 1990; Vol. 1.
44. Coats, D.; Greenfield, S.; Sage, I. C.; Smith, G. Proc SPIE 1990, 37, 1257.
45. Kim, B. K.; Ok, Y. S. J Appl Polym Sci 1993, 49, 1769.
46. Kikuchi, H.; Nishiwaki, J.; Kajiyama, T. Polym J 1995, 12, 1246.
47. Choi, C. H.; Kim, B. K.; Kikuchi, H.; Kajiyama, T.; Amaya, N.; Murata, Y. J Appl Polym Sci 1994, 50, 2217.
48. Choi, C. H.; Kim, S. H.; Hong, E. V.; Kim, B. K. Eur Polym J 1997, 33, 565.
49. Kim, S. H.; Heo, Z. C. P.; Park, K. S.; Kim, B. K. Polym Int 1998, 46, 143.